Biophysical Journal
Article

Biophysical Society

A Dynamical Threshold for Cardiac Delayed Afterdepolarization-Mediated Triggered Activity

Michael B. Liu,[1,2] Christopher Y. Ko,[1,2] Zhen Song,[1,2] Alan Garfinkel,[1,2,3] James N. Weiss,[1,2,4] and Zhilin Qu[1,2,5,*]
[1]Cardiovascular Research Laboratory, [2]Department of Medicine, [3]Department of Integrative Biology and Physiology, [4]Department of Physiology, and [5]Department of Biomathematics, David Geffen School of Medicine, University of California, Los Angeles, Los Angeles, California

ABSTRACT Ventricular myocytes are excitable cells whose voltage threshold for action potential (AP) excitation is ~−60 mV at which I_{Na} is activated to give rise to a fast upstroke. Therefore, for a short stimulus pulse to elicit an AP, a stronger stimulus is needed if the resting potential lies further away from the I_{Na} threshold, such as in hypokalemia. However, for an AP elicited by a long duration stimulus or a diastolic spontaneous calcium release, we observed that the stimulus needed was lower in hypokalemia than in normokalemia in both computer simulations and experiments of rabbit ventricular myocytes. This observation provides insight into why hypokalemia promotes calcium-mediated triggered activity, despite the resting potential lying further away from the I_{Na} threshold. To understand the underlying mechanisms, we performed bifurcation analyses and demonstrated that there is a dynamical threshold, resulting from a saddle-node bifurcation mainly determined by I_{K1} and I_{NCX}. This threshold is close to the voltage at which I_{K1} is maximum, and lower than the I_{Na} threshold. After exceeding this dynamical threshold, the membrane voltage will automatically depolarize above the I_{Na} threshold due to the large negative slope of the I_{K1}-V curve. This dynamical threshold becomes much lower in hypokalemia, especially with respect to calcium, as predicted by our theory. Because of the saddle-node bifurcation, the system can automatically depolarize even in the absence of I_{Na} to voltages higher than the $I_{Ca,L}$ threshold, allowing for triggered APs in single myocytes with complete I_{Na} block. However, because I_{Na} is important for AP propagation in tissue, blocking I_{Na} can still suppress premature ventricular excitations in cardiac tissue caused by calcium-mediated triggered activity. This suppression is more effective in normokalemia than in hypokalemia due to the difference in dynamical thresholds.

INTRODUCTION

Under normal conditions, ventricular myocytes have a diastolic resting potential at ~−80 mV, stabilized by the inward rectifier K^+ current (I_{K1}). An action potential (AP) can be elicited by a brief current pulse, overcoming the stabilizing effect of I_{K1} and bringing the voltage to the threshold (~−60 mV) for Na^+ current (I_{Na}) activation. In other words, the voltage threshold for eliciting an AP using a brief stimulus pulse is near the I_{Na} threshold at ~−60 mV for a ventricular myocyte. Therefore, when the resting potential is hyperpolarized (e.g., under hypokalemic conditions), a larger stimulus current for a brief pulse is needed to depolarize the membrane voltage to the I_{Na} threshold to elicit an AP. Similarly, the conduction velocity in cardiac tissue is slower for a hyperpolarized resting potential (1–3). The resting potential of a ventricular myocyte can also be destabilized by reduction of I_{K1} to result in pacemaking activity (4,5) or delayed afterdepolarization (DAD)-mediated triggered activity (TA) (6–8). In both cases, a lowered I_{K1} allows the Na^+-Ca^{2+} exchange current (I_{NCX}) to overcome the repolarizing effect of I_{K1}, depolarizing the cell to the I_{Na} threshold for AP generation.

A DAD is a voltage depolarization caused by spontaneous calcium (Ca^{2+}) release (SCR) during the diastolic phase after a previous AP (9–13). If the depolarization is large enough to reach the I_{Na} threshold, the DAD can trigger an AP causing TA. This phenomenon is potentiated by various diseased conditions including heart failure (7,14) and hypokalemia (15). In heart failure, ryanodine receptors become leaky, which promotes SCRs resulting in DADs. In addition, I_{K1} is reduced and I_{NCX} is increased, which decreases the diastolic Ca^{2+}-to-voltage gain to promote TA.

In hypokalemia, multiple factors come into play. Na^+-K^+ pump activity is reduced, which results in an elevated intracellular Na^+ concentration (16,17). This inhibits forward Na^+-Ca^{2+} exchange, which increases intracellular Ca^{2+} concentration and promotes SCR. Hypokalemia also causes

Submitted May 12, 2016, and accepted for publication October 11, 2016.
*Correspondence: zqu@mednet.ucla.edu
Michael B. Liu and Christopher Y. Ko contributed equally to this article.
Editor: Godfrey Smith.
http://dx.doi.org/10.1016/j.bpj.2016.10.009

a reduced I_{K1} conductance, which tends to destabilize the resting potential and potentiates DAD-mediated TA. However, hypokalemia also causes a hyperpolarized resting potential through the left shift of reversal potential E_K. This acts to move the membrane voltage further away from the I_{Na} threshold, which would seem to counter the TA-promoting effect of reduced I_{K1}.

A recent theoretical study by Greene and Shiferaw (18) showed that the voltage threshold for DAD-mediated TA is actually lower than the I_{Na} threshold, and is determined by the voltage at which I_{K1} is maximal. These findings indicate that the traditional understanding of the voltage threshold for DAD-mediated TA as the voltage threshold for I_{Na} activation needs to be revisited. In this study, we seek to dissect the determinants of the threshold for DAD-mediated TA in normokalemic and hypokalemic conditions, using patch-clamp experiments, computer simulations, and nonlinear dynamics. We show that there exists a dynamical threshold for TA, which is a saddle-node bifurcation point, mainly determined by I_{K1} and I_{NCX}. This threshold becomes lower in hypokalemia, potentiating DAD-mediated TA in hypokalemia.

MATERIALS AND METHODS

Myocyte experiments

Ventricular myocyte isolation

Young adult (3–4 months of age) New Zealand white male rabbits (1.7–2.0 kg) were euthanized by intravenous injection of heparin sulfate (1000 U) and sodium pentobarbital (100 mg/kg). Hearts were quickly excised by thoracotomy and retrogradely perfused at 37°C in Langendorff fashion with Ca^{2+}-free Tyrode's solution for 5–7 min followed by enzyme digestion perfusion with Tyrode's solution containing 0.05 mg/mL Liberase TH (Roche, South San Francisco, CA) for 20–30 min at 25 mL/min. The Tyrode's solution contained the following: 136 mmol/L NaCl, 5.4 mmol/L KCl, 0.33 mmol/L NaH_2PO_4, 1.0 mmol/L $MgCl_2$, 10 mmol/L HEPES, and 10 mmol/L glucose (pH 7.4 with KOH). All chemicals were purchased from Sigma-Aldrich (St. Louis, MO) unless indicated otherwise. Myocytes were separated from digested ventricles by gentle mechanical dissociation in 0.2 mM Ca^{2+} Tyrode's solution. Ca^{2+} concentration was gradually increased to 1.8 mmol/L over 30 min. Myocytes were used within 6–8 h. All procedures complied with UCLA Animal Research Committee policies.

Patch-clamp experiments in myocytes

Standard whole-cell patch-clamp methods were used to measure voltage in the current-clamp mode. Borosilicate glass electrodes (tip resistance 1.4–2.2 MΩ) were filled with internal solution containing 110 mmol/L K-Aspartate, 30 mmol/L KCl, 5 mmol/L NaCl, 10 mmol/L HEPES, 5 mmol/L MgATP, 5 mmol/L creatine phosphate, 1 mmol/L KH_2PO_4, and 0 mmol/L EGTA (pH 7.2 with KOH). All chemicals were purchased from Sigma-Aldrich unless indicated otherwise. Data were acquired with an Axopatch 200A patch-clamp amplifier and Digidata 1200 acquisition board driven by pCLAMP 9.0 software (Axon Instruments, Union City, CA). Corrections were made for liquid junction potentials. Signals were filtered at 1 kHz. All experiments were carried out in Tyrode's solution maintained at 37°C. Constant current square pulses (2 or 200 ms duration) were applied stepwise in 0.1 nA increments from −0.2 nA up to 3.0 nA to determine AP thresholds under normokalemic ($[K^+]_o = 5.4$ mM) or hypokalemic ($[K^+]_o = 2.7$ mM) conditions. For experiments involving Na^+ channel blockade, patch-clamped myocytes were rapidly superfused with either normal Tyrode's solution or Tyrode's solution containing 20 μmol/L tetrodotoxin (TTX) (Tocris Bioscience, Bristol, UK) using a rapid solution exchange device (19) positioned near the myocyte under the control of Axopatch software (Axon Instruments).

Computer simulations

Computer simulations were performed in a single cell and one-dimensional (1D) cables using the AP model previously described by Mahajan et al. (20). In the single-cell simulations, the cell model was first prepaced to its steady state. Spontaneous Ca^{2+} releases were simulated by clamping the myocyte submembrane Ca^{2+} ($[Ca^{2+}]_s$) level to a Gaussian-like shape during the diastolic phase after a stimulated AP, i.e., $[Ca^{2+}]_s = Ca_{peak} \times e^{-(t-t_0)^2/2\sigma^2}$, where t_0 is the peak time of $[Ca^{2+}]_s$ (t was set to zero at the time of the stimulation; see Fig. 1), σ determines the width of the Ca^{2+} transient, and Ca_{peak} is the peak $[Ca^{2+}]_s$ value. σ = 150 ms and t_0 = 850 ms were used for all simulations unless otherwise specified. Submembrane Ca^{2+} was used to determine Ca^{2+} thresholds to produce a DAD of sufficient amplitude to cause TA, because the I_{NCX} dependence on Ca^{2+} is specifically formulated in terms of submembrane Ca^{2+}. Normokalemia and hypokalemia were simulated by changing the value of $[K^+]_o$ from 5.4 to 2.7 mM. Intracellular sodium ($[Na^+]_i$) was clamped to 10 mM.

One-dimensional cable simulations were carried out using the following equation for voltage:

$$\frac{\partial V}{\partial t} = -I_{ion}/C_m + D\left(\frac{\partial^2 V}{\partial x^2}\right), \quad (1)$$

where V is the membrane voltage, C_m = 1 μF/cm^2 is the membrane capacitance, and D is the diffusion constant set to 0.0005 cm^2/ms. The prepaced single-cell steady state was used as initial condition for each cell in the cable. DADs were simulated by a time-dependent commanded spontaneous release of the SR Ca^{2+} with random latencies drawn from a Gaussian distribution with a certain standard deviation as described in Xie et al. (21) and

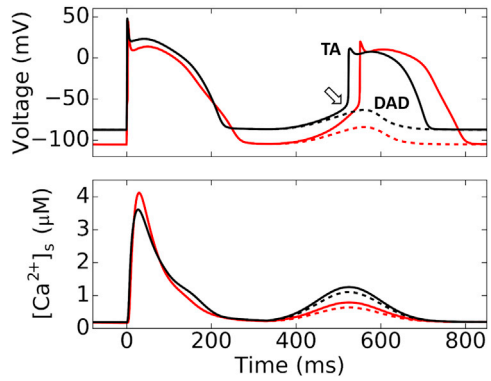

FIGURE 1 Simulated DAD and TA using the AP model. Membrane voltage (*upper traces*) and submembrane Ca^{2+} concentration ($[Ca^{2+}]_s$, *lower traces*) during a normal stimulated AP followed by a DAD due to spontaneous Ca^{2+} release which is just above (*solid lines*) or below (*dashed lines*) the threshold to trigger an AP. (*Black traces*) Normokalemia ($[K^+]_o$ = 5.4 mM); (*red traces*) hypokalemia ($[K^+]_o$ = 2.7 mM). (*Open arrow*) I_{Na} threshold. The parameters for Gaussian-like function of the clamped spontaneous Ca^{2+} release (see Materials and Methods) were t_0 = 525 ms and σ = 70 ms for all four traces. For normokalemia, Ca_{peak} = 1.258 μM (*black solid*) and 1.102 μM (*black dashed*), respectively. For hypokalemia, Ca_{peak} = 0.79 μM (*red solid*) and 0.634 μM (*red dashed*). To see this figure in color, go online.

Liu et al. (22). Briefly, a SR release conductance was added with a certain strength and duration to release Ca^{2+} from the SR. The onset of this release was determined by a random latency drawn from the Gaussian distribution. A time adaptive algorithm was used with a time step (Δt) varying between 0.01 ms and 0.1 ms. In the single-cell simulations, DAD-mediated triggered activity was considered to have occurred if the voltage exceeded 0 mV. In the cable simulations, if a propagating wave was detected at either end of the cable after the sinus beat, a propagating premature ventricular contraction (PVC) was considered to have occurred.

RESULTS

Hypokalemia results in a lower threshold for DAD-mediated TA in a ventricular myocyte model

We carried out simulations to examine the threshold for TA in the rabbit ventricular myocyte model by Mahajan et al. (20). The spontaneous Ca^{2+} release that causes a DAD or TA was simulated by a clamped Ca^{2+} transient (see Materials and Methods). Fig. 1 shows the voltage and $[Ca^{2+}]_s$ for a stimulated beat followed by a spontaneous Ca^{2+} release just below (*dashed*) and above (*solid*) the threshold for TA. Hypokalemia hyperpolarized the resting membrane potential to <-100 mV. Despite the resting potential being 20 mV more negative, the Ca^{2+} amplitude threshold for DAD-mediated TA is much lower during hypokalemia than normokalemia, indicating that hypokalemia substantially lowers the threshold for TA. This is consistent with well-known experimental observations that hypokalemia potentiates DAD-mediated TA despite hyperpolarizing the resting membrane potential (15). The voltage still needs to eventually depolarize past the I_{Na} threshold to result in a fast upstroke under both normokalemia and hypokalemia. However, in the case of hypokalemia, a much smaller Ca^{2+} transient and thus a much smaller I_{NCX} was sufficient to depolarize the voltage to the same I_{Na} threshold. To gain a more complete understanding of the mechanisms underlying this phenomenon, we combined nonlinear dynamics analysis with computer simulations and patch-clamp experiments as described in the sections below.

Short and long current pulse thresholds for eliciting an AP

Because the duration of a DAD is much longer than that of a typical electrical stimulus, we first studied the role that the duration of a pulse stimulus plays in eliciting an AP. Fig. 2 compares excitation thresholds for a short (2 ms) versus a long (200 ms) current pulse to elicit an AP in a patch-clamped rabbit ventricular myocyte (current clamp mode) under both normokalemic ($[K]_o = 5.4$ mM) and hypokalemic conditions ($[K]_o = 2.7$ mM). Hypokalemia shifted the resting potential from -87 to -110 mV.

For the 2 ms current pulse (Fig. 2, *A* and *B*), the minimum current required to elicit an AP increased from 1.6 nA under normokalemic conditions to 2.1 nA under hypokalemic conditions, as expected due to the more hyperpolarized resting membrane potential during hypokalemia. In both cases, the smallest current amplitude eliciting an AP depolarized the membrane very close to the I_{Na} threshold of -60 mV, followed by the AP upstroke within 5 ms. For the 200 ms current pulse (Fig. 2, *C* and *D*), however, the results were reversed, with the minimum current eliciting an AP decreasing from 0.6 nA during normokalemia to 0.5 nA

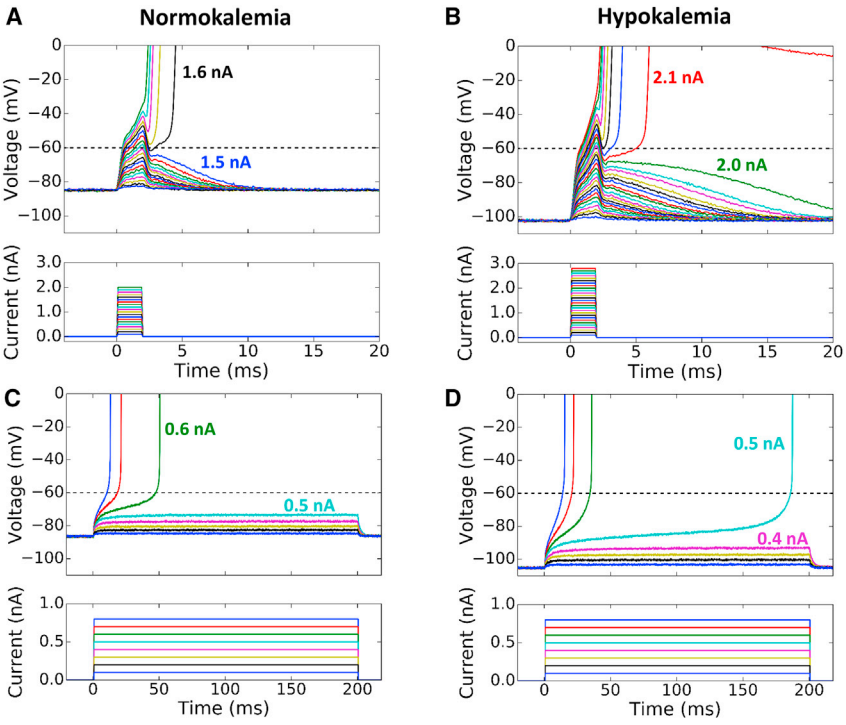

FIGURE 2 Current thresholds for triggering an AP by short and long stimuli in normokalemic ($[K^+]_o = 5.4$ mM) and hypokalemic ($[K^+]_o = 2.7$ mM) rabbit ventricular myocytes. (*A*) Superimposed voltage (*upper*) and current (*lower*) traces during 2 ms current pulses of increasing amplitude in a normokalemic patch-clamped rabbit ventricular myocyte. The minimum current needed to elicit an AP was 1.6 nA. (*B*) Same as (*A*), but during hypokalemia. With a hyperpolarized resting potential, the minimum current needed to elicit an AP increased to 2.1 nA. (*C* and *D*) Corresponding traces for 200 ms current pulses. The minimum current needed to elicit an AP was 0.6 nA, which decreased to 0.5 nA during hypokalemia. Note how the take-off potential is lower than the I_{Na} activation threshold at -60 mV, and is further lowered in hypokalemia. To see this figure in color, go online.

during hypokalemia. Moreover, the smallest current amplitude eliciting an AP initially depolarized the membrane voltage to only −74 mV for normokalemia and −94 mV for hypokalemia. The membrane voltage then rose very slowly before finally reaching the I_{Na} activation threshold at ~−60 mV to generate the AP upstroke. Thus, consistent with the predictions from Greene and Shiferaw (18), the threshold for a long current pulse to elicit an AP was considerably more negative than −60 mV, especially during hypokalemia.

To analyze the dynamics underlying these behaviors, we considered a system composed only of I_{K1} and the stimulus current (I_{sti}), described by the following differential equation:

$$\frac{dV}{dt} = -(I_{K1} + I_{sti})/C_m, \tag{2}$$

where I_{sti} is a square pulse with a duration (τ) and height (I_0), i.e.,

$$I_{sti} = \begin{cases} -I_0, & 0 \le t \le \tau \\ 0, & t > \tau, \end{cases} \tag{3}$$

The resting potential of Eq. 2 is simply the reversal potential (E_K) of I_{K1}. The voltage at the end of the stimulus current pulse ($t = \tau$) is given by

$$V(\tau) = \int_0^{\tau} -(I_{K1} - I_0)/C_m dt. \tag{4}$$

To facilitate analytical solutions of Eqs. 2 or 4, we approximated I_{K1} by a piecewise linear function as follows (Fig. 3 *A*):

$$I_{K1} = \begin{cases} \alpha(V - E_K), & V < V_{max} \\ \beta(V_0 - V), & V_{max} \le V \le V_0 \\ 0 & V > V_0, \end{cases} \tag{5}$$

where $\alpha = I_{K1,max}/V_{max} - E_K$ and $\beta = I_{K1,max}/V_0 - V_{max}$. $I_{K1,max}$ is the peak I_{K1} at V_{max}. V_{max} and V_0 are defined as in Fig. 3 *A*.

When $I_0 < I_{K1,max}$, Eq. 4 can be explicitly solved, which leads to

$$V(\tau) = E_K + \frac{I_0}{\alpha} - \frac{I_0}{\alpha} e^{-\frac{\alpha\tau}{C_m}}. \tag{6}$$

For an infinitely long pulse, the voltage reaches a steady state, which is given by

$$V(\tau \to \infty) = E_K + \frac{I_0}{\alpha} < V_{max}. \tag{7}$$

When $I_0 > I_{K1,max}$, the solution of Eq. 2 can be expressed with three time regions as follows:

1) For $t < t'$,

$$V(t) = E_K + \frac{I_0}{\alpha} - \frac{I_0}{\alpha} e^{-\frac{\alpha t}{C_m}}, \tag{8}$$

with t' as the time at which $V(t') = V_{max}$, obtained from Eq. 8 as

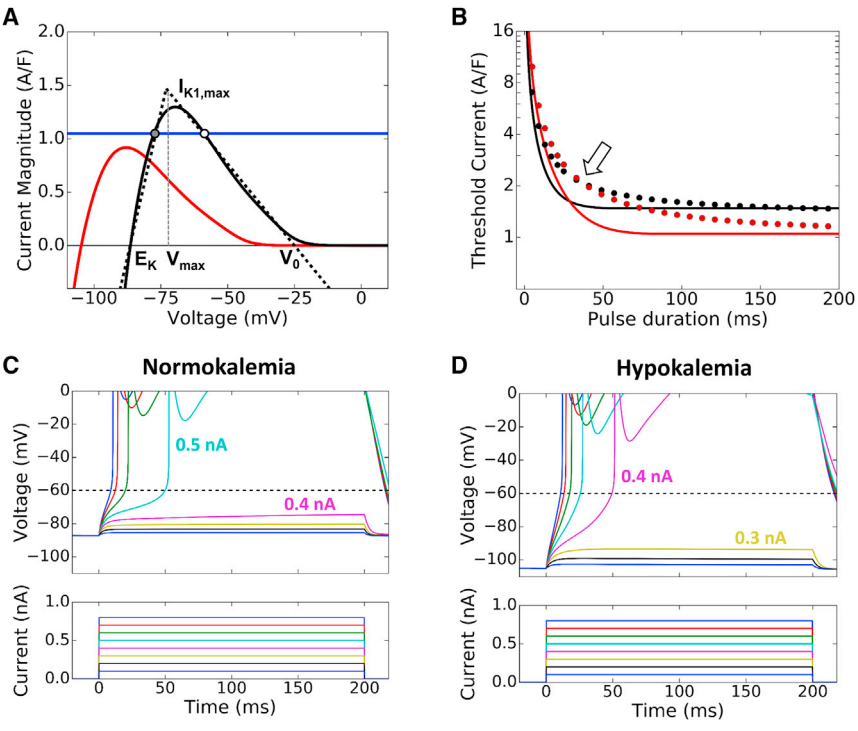

FIGURE 3 Theoretical analysis of the current threshold for triggering an AP by a pulse stimulus. (*A*) The I_{K1}-V curves for normokalemia ($[K^+]_o$ = 5.4 mM, *black*) and hypokalemia ($[K^+]_o$ = 2.7 mM, *red*). The I_{K1} curve is mainly determined by four parameters: E_K, $I_{K1,max}$, V_{max}, and V_0. To most closely match the actual I_{K1} curves, for normokalemia we used E_K = −86.5 mV, $I_{K1,max}$ = 1.47 A/F, V_{max} = −73 mV, and V_0 = −25 mV. For hypokalemia, we used E_K = −104.5 mV, $I_{K1,max}$ = 1.04 A/F, V_{max} = −92 mV, and V_0 = −43 mV in the linear piecewise approximation for I_{K1} (*dotted line*) used for the analytical treatment. (*Blue horizontal line*) Example of constant inward current that is subthreshold in normokalemia but suprathreshold in hypokalemia. (*Circles*) Points at which the net current is zero, i.e., the equilibrium points. (*Solid circle*) Stable equilibrium point; (*open circle*) unstable equilibrium point in normokalemia. In hypokalemia, this example has no equilibrium point. (*B*) The threshold current ($I_{0,th}$) versus pulse duration (τ) from the theoretical prediction (*lines*), and from the simulations (*dots*) using the AP model with a constant stimulus pulse of varying duration in normokalemia (*black*) and hypokalemia (*red*). (*Open arrow*) Where the current threshold reverses between normokalemia and hypokalemia. (*C* and *D*) Voltage (*upper*) and current (*lower*) traces corresponding to 200 ms current pulses of increasing amplitude during normokalemia and hypokalemia, from the simulations using the AP model. The minimum current needed to elicit an AP was 0.5 nA, which decreased to 0.4 nA in simulated hypokalemia. Note again how the takeoff potential is lower than the I_{Na} activation threshold, and is further lowered in hypokalemia. To see this figure in color, go online.

$$t' = -\frac{C_m}{\alpha}\ln\frac{-\left(V_{\max} - \mathrm{E_K} - \frac{\mathrm{I_0}}{\alpha}\right)\alpha}{\mathrm{I_0}}. \quad (9)$$

2) For $t' < t < t''$,

$$V(t) = V_0 - \frac{I_0}{\beta} + \left(V_{\max} - V_0 + \frac{\mathrm{I_0}}{\beta}\right)e^{\frac{\beta(t-t')}{C_m}}, \quad (10)$$

with t'' as the time at which $V(t'') = V_0$, obtained from Eq. 10 as

$$t'' = t' + \frac{C_m}{\beta}\ln\frac{\frac{\mathrm{I_0}}{\beta}}{V_{\max} - V_0 + \frac{\mathrm{I_0}}{\beta}}. \quad (11)$$

3) For $t > t''$,

$$V(t) = V_0 + \mathrm{I_0}(t - t'')C_m. \quad (12)$$

Because the $\mathrm{I_{Na}}$ threshold ($V_{\mathrm{th,Na}}$) is near −60 mV, which is higher than $V_{\max}$ but lower than V_0 (see Fig. 3 *A*), then only the cases where $t < t''$ needs to be considered. Assume that at $t = \tau$, the voltage reaches the $\mathrm{I_{Na}}$ threshold, i.e., $V(\tau) = V_{\mathrm{th,Na}}$. Equation 10 then becomes

$$V_{\mathrm{th,Na}} = V_0 - \frac{\mathrm{I_{0,th}}}{\beta} + \left(V_{\max} - V_0 + \frac{\mathrm{I_{0,th}}}{\beta}\right)e^{\frac{\beta(\tau-t')}{C_m}}, \quad (13)$$

which leads to

$$\tau = t' + \frac{C_m}{\beta}\ln\frac{V_{\mathrm{th,Na}} - V_0 + \frac{\mathrm{I_{0,th}}}{\beta}}{V_{\max} - V_0 + \frac{\mathrm{I_{0,th}}}{\beta}}. \quad (14)$$

By inserting t' from Eq. 9 to Eq. 14, one obtains

$$\tau = \frac{C_m}{\beta}\ln\frac{V_{\mathrm{th,Na}} - V_0 + \frac{\mathrm{I_{0,th}}}{\beta}}{V_{\max} - V_0 + \frac{\mathrm{I_{0,th}}}{\beta}} - \frac{C_m}{\alpha}\ln\frac{-\left(V_{\max} - E_K - \frac{\mathrm{I_{0,th}}}{\alpha}\right)\alpha}{\mathrm{I_{0,th}}}. \quad (15)$$

By setting $\tau = \infty$ in Eq. 15 (this can only be satisfied if the second logarithmic term goes to infinity), the minimum stimulus strength can be calculated as

$$\mathrm{I_{0,th}} = \alpha\,(V_{\max} - \mathrm{E_K}) = \mathrm{I_{K1,max}}. \quad (16)$$

Therefore, when $\mathrm{I_{0,th}} < \mathrm{I}_{K1,\max}$, the voltage can never reach $V_{\mathrm{th,Na}}$ but rather asymptotically approaches the steady state (Eq. 7), which is always lower than $V_{\max}$. However, when $\mathrm{I_{0,th}} > \mathrm{I_{K1,max}}$, there always exists a finite τ during which the voltage can grow to reach $V_{\mathrm{th,Na}}$.

Hypokalemia has three main effects on $\mathrm{I_{K1}}$: a left shift of $\mathrm{E_K}$; a left shift of $V_{\max}$; and a reduced $\mathrm{I_{K1,max}}$, as shown in Fig. 3 *A*.

In Fig. 3 *B*, we plot the threshold current $\mathrm{I_{0,th}}$ versus the pulse duration τ using Eq. 15 for both normokalemia and hypokalemia, showing that $\mathrm{I_{0,th}}$ is smaller for normokalemia than for hypokalemia when $\tau < 29$ ms, which is reversed when $\tau > 29$ ms. We also plot in Fig. 3 *B* the corresponding results (*circles*) from the computer simulation using the rabbit ventricular myocyte model, which agrees well with the theoretical prediction. Fig. 3, *C* and *D*, shows two examples of incremental current amplitudes with a 200 ms pulse duration to illustrate the threshold current in normokalemia ($[\mathrm{K^+}]_o = 5.4$ mM) and hypokalemia ($[\mathrm{K^+}]_o = 2.7$ mM).

Based on Eqs. 15 and 16, the threshold current $\mathrm{I_{0,th}}$ to elicit an AP depends on the voltage threshold of the $\mathrm{Na^+}$ channel ($V_{\mathrm{th,Na}}$) for a short stimulus pulse but not for a long pulse. This indicates that in the absence of $\mathrm{Na^+}$ current ($\mathrm{I_{Na}}$), a larger $\mathrm{I_{0,th}}$ is required to elicit an AP for a short pulse because the voltage threshold ($V_{\mathrm{th,Ca}}$) for L-type $\mathrm{Ca^{2+}}$ channel is higher (~−40 mV). For a long pulse, $\mathrm{I_{0,th}}$ will remain unchanged because Eq.16 is independent of either $V_{\mathrm{th,Na}}$ or $V_{\mathrm{th,Ca}}$. To demonstrate this experimentally, we performed patch-clamp experiments as in Fig. 2 by blocking the $\mathrm{Na^+}$ channel using TTX (Fig. 4). For a 2 ms stimulation pulse, the addition of TTX increased the current threshold from 1.8 to 2.5 nA (Fig. 4, *A* and *B*). However, for a 200 ms stimulation pulse, the addition of TTX did not change the current threshold, which remained at 0.7 nA before and after TTX addition (Fig. 4, *C* and *D*), agreeing with the theoretical prediction. Note that after TTX application, the turning points for steep upstroke occurred at higher voltages and the maximum upstroke slopes were reduced under both short and long pulses (see corresponding *dV/dt* plots in the *insets*). This indicates that TTX was effective in blocking the $\mathrm{Na^+}$ channel and the AP upstroke after TTX was mediated by the L-type $\mathrm{Ca^{2+}}$ current ($\mathrm{I_{Ca,L}}$). Based on our theory, this same observation should hold true for hypokalemia. However, the TTX effect of blocking the $\mathrm{Na^+}$ channel is voltage dependent, which becomes less effective for lower preholding voltages (23–25). Because of this voltage-dependent behavior, we were not able to convincingly repeat this experimental protocol in hypokalemia.

Nonlinear dynamics caused by the interaction of $\mathrm{I_{K1}}$ and $\mathrm{I_{NCX}}$

In contrast to constant current pulses, the depolarizing current $\mathrm{I_{NCX}}$ during a DAD is not constant, but a function of $\mathrm{Na^+}$, $\mathrm{Ca^{2+}}$, and voltage. Therefore, the analysis for constant current pulses above provides important qualitative insights, but it is not sufficient for a detailed understanding of the mechanisms of DAD-mediated TA. Here we further analyze

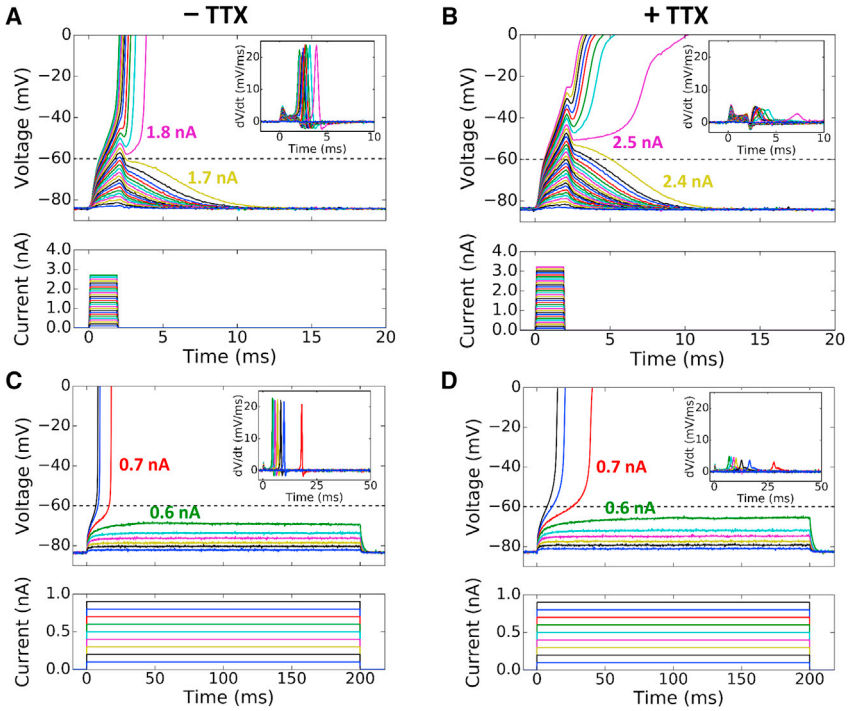

FIGURE 4 Current thresholds for triggering an AP by short and long stimuli with and without TTX. (*A*) Superimposed voltage (*upper*) and current (*lower*) traces during 2 ms current pulses of increasing amplitude in a normokalemic patch-clamped rabbit ventricular myocyte (repeat of the protocol in Fig. 2 *A* in a different cell). The minimum current needed to elicit an AP was 1.8 nA. (*Inset*) Rate of change of the voltage traces (*dV/dt*). (*B*) Same as (*A*) but in the presence of 20 μM TTX. With the addition of TTX, the minimum current needed to elicit an AP increased to 2.5 nA. (*Inset*) Fourfold reduction in maximum *dV/dt* due to TTX. (*C* and *D*) Corresponding traces for 200 ms current pulses without and with TTX, respectively. The minimum current needed to elicit an AP was 0.7 nA in both cases, demonstrating no change in the current threshold by TTX. Again, the addition of TTX reduced the *dV/dt*. To see this figure in color, go online.

the nonlinear dynamical interactions between I_{K1} and I_{NCX} using the following equation:

$$\frac{dV}{dt} = -(I_{K1} + I_{NCX})/C_m. \tag{17}$$

For simplicity, we first assume Na^+ and Ca^{2+} to be constant parameters instead of changing variables, and thus Eq. 17 is a nonlinear equation with respect to voltage only. At equilibrium, $dV/dt = 0$, which leads to

$$I_{K1} = -I_{NCX}, \tag{18}$$

i.e., when the magnitudes of the two currents are equal, the system is at an equilibrium point.

Because the currents involved are nonlinear functions of voltage, multiple equilibria can exist. Fig. 5 *A* plots the I-V curves for I_{K1} and inverted I_{NCX} ($-I_{NCX}$), in which the intersections of the two curves are the equilibrium points. When Ca^{2+} is low, I_{NCX} is small and there is only one intersection close to the reverse potential of I_{K1} (E_K). The net current is inward when voltage is more negative than the equilibrium point and outward when voltage is more positive (*top panel* in Fig. 5 *B*). Therefore, if the voltage is displaced away from the equilibrium voltage, it is automatically driven back toward the equilibrium point, and thus the equilibrium point is stable. As Ca^{2+} rises, the $-I_{NCX}$ curve increases and shifts to the right, resulting in three equilibrium points. The total net current changes from inward to outward, then to inward, and to outward again as voltage increases (*middle panel* in Fig. 5 *B*). Thus the lower and upper equilibrium points are stable while the middle is unstable. As Ca^{2+} rises above a critical level, the lower equilibria points converge then vanish, leaving only the single stable high voltage equilibrium point remaining. This behavior is summarized in Fig. 5 *C* by plotting the equilibrium voltages of this two-current system versus Ca^{2+} concentration, with the stable equilibrium points plotted as a solid line and unstable points as a dashed line. Therefore, when Ca^{2+} exceeds a critical value (*arrows* in Fig. 5 *C*), the membrane voltage will automatically depolarize toward the remaining single equilibrium point at high voltage. This occurs because of the steep negative slope of the I_{K1}-V curve in this region causing I_{K1} to decrease faster than $-I_{NCX}$ as voltage increases, making the net current always inward, thereby depolarizing the membrane voltage further. The voltage at the critical point, which occurs where the $-I_{NCX}$ curve lies exactly tangent to I_{K1} slightly above V_{max}, is lower than the I_{Na} threshold. Therefore, once the voltage reaches this critical value, it will continue to rise. We call this critical voltage a dynamical threshold because it is determined by the nonlinear dynamics of the interaction between I_{K1} and I_{NCX}. The dynamical threshold is a bifurcation point called a saddle-node bifurcation point (26). Hypokalemia results in a lower voltage threshold (*red line* in Fig. 5 *C*) due to the left shift of the I_{K1}-V curve and reduction of maximum I_{K1} conductance.

Influence of the intracellular Ca^{2+} waveform during spontaneous Ca^{2+} release on AP activation

The nonlinear dynamics shown in Fig. 5 is valid when Ca^{2+} is constant, but during a DAD, cytosolic Ca^{2+} concentration

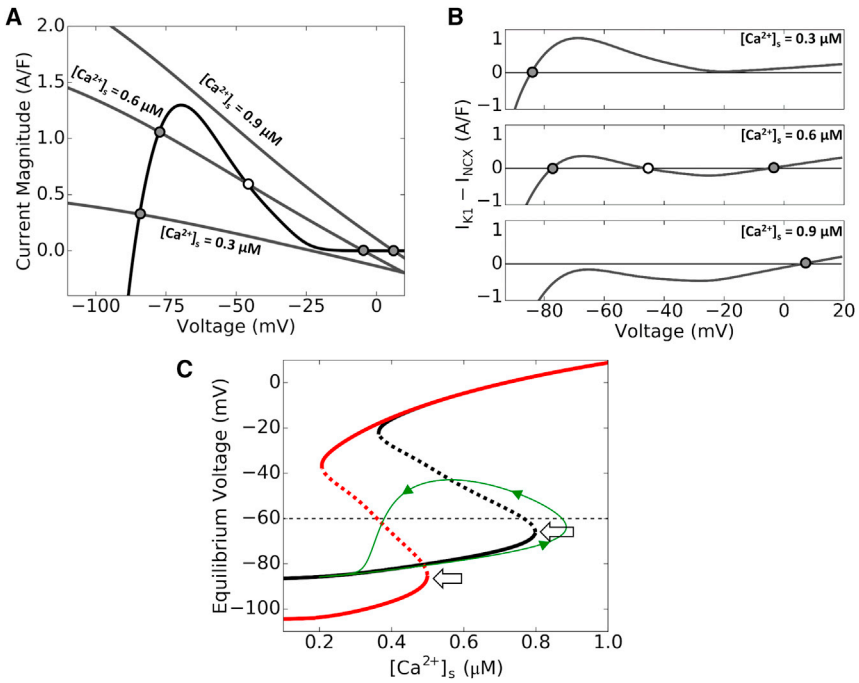

FIGURE 5 A dynamical threshold determined by I_{K1} and I_{NCX} for a constant Ca^{2+} condition. (*A*) I-V plot of I_{K1} and $-I_{NCX}$ at $[K]_o$ = 5.4 mM (normokalemia), corresponding to low (0.3 μM), medium (0.6 μM), and high (0.9 μM) submembrane Ca^{2+} concentration levels. (*Solid circles*) Stable equilibrium points; (*open circle*) unstable equilibrium point. Note how with low Ca^{2+} there is only one (stable) equilibrium point at low voltage, with medium Ca^{2+} there are three (stable-unstable-stable) equilibrium points, and with high Ca^{2+} there is only one (stable) equilibrium point at high voltage. (*B*) Net current versus voltage for the corresponding three cases in (*A*), using the same symbols for the equilibrium points. (*C*) Equilibrium voltage versus steady-state Ca^{2+} during normokalemia (*black*) and hypokalemia (*red*). (*Solid lines*) Stable equilibrium points; (*dashed lines*) unstable equilibrium points for the particular Ca^{2+} concentration. (*Arrows*) Respective dynamical thresholds, which determine the voltage and Ca^{2+} needed to cross the saddle-node and elicit an AP. (*Green trace*) Example of a simulated trajectory using the simple two-current system consisting of I_{K1} and I_{NCX}, with a Ca^{2+} transient simulated by a Gaussian-shaped function similar to the function described in Fig. 1. Note that voltage continues to increase for a period of time even after the Ca^{2+} concentration has started to decrease, due to crossing the dynamical threshold. To see this figure in color, go online.

rises and then falls. As Ca^{2+} increases from the diastolic Ca^{2+} concentration, the system first follows the lower branch of equilibrium voltage. When Ca^{2+} increases past the critical value (*arrows* in Fig. 5 *C*), voltage will continue to increase even when Ca^{2+} is declining (*green trajectory* in Fig. 5 *C*). Therefore, whether a cell reaches the I_{Na} threshold to trigger an AP depends not only on crossing the dynamical threshold, but also on the rate of decay of Ca^{2+} influencing the I_{NCX} curve. To investigate the effects of Ca^{2+} decay on the TA threshold, we varied the duration of a clamped Ca^{2+} transient with a Gaussian-like shape by changing the width of full width at half-maximum (FWHM). Fig. 6 *A* shows the Ca^{2+} transient amplitude threshold for TA (i.e., the peak amplitude of the Ca^{2+} transient required to trigger an AP) versus the width of the Ca^{2+} transient for different values of $[K^+]_o$. The Ca^{2+} transient amplitude threshold for TA decreased with lower $[K^+]_o$ or a wider Ca^{2+} transient that decays more slowly. The dependence of the Ca^{2+} threshold on Ca^{2+} transient width gradually saturates when the Ca^{2+} transient FWHM is >~200 ms. This indicates that when the Ca^{2+} transient duration is 200 ms or longer, the system has reached the steady-state solution, closely agreeing with the prediction of the bifurcation analysis, when including I_{NaK}, which contributes ~20% to the effective I_{K1} peak (*dashed lines* in Fig. 6 *A*). The FWHM was observed in rabbit ventricular myocytes to be 180–300 ms (27), which easily satisfies this condition and therefore are always in the regime of the dynamical threshold.

As I_{NCX} and I_{NaK} both depend on the intracellular Na^+ concentration of the myocyte, we investigated the effect of $[Na^+]_i$ on the TA threshold. Fig. 6 *B* shows that lower $[Na^+]_i$ lowers the TA threshold, while higher $[Na^+]_i$ increases the threshold. This can be explained by the two diastolic currents that $[Na^+]_i$ affects: I_{NaK} and I_{NCX}. At higher $[Na^+]_i$, I_{NaK} contributes to a slightly higher effective I_{K1} peak through the I_{NaK} contribution, while I_{NCX} is reduced. Both of these factors would serve to make TA more difficult, requiring a higher Ca^{2+} transient amplitude. With lower $[Na^+]_i$ the opposite occurs, with I_{NaK} resulting in a slightly lower effective I_{K1} peak with increased I_{NCX}, allowing TA to occur more easily at a lower Ca^{2+} transient amplitude. Note that these simulations only studied the effect of changing $[Na^+]_i$ with a given Ca^{2+} transient, and did not take into account any Ca^{2+} loading effects caused by the changes in $[Na^+]_i$.

Finally, to sort out the effects of lowered resting potential and reduced I_{K1} conductance caused by hypokalemia, we carried out simulations under four conditions: 1) control (normokalemia); 2) reduced I_{K1} conductance only; 3) left shift of I_{K1} through E_K only; and 4) both reduced I_{K1} conductance and left shift of E_K (hypokalemia). Fig. 6 *C* shows the steady-state equilibrium voltage versus Ca^{2+} obtained using the simple system described by only I_{K1} and I_{NCX} (Eq. 17), which shows that the reduction of I_{K1} conductance and the left shift of E_K alone both resulted in similar lowered Ca^{2+} and voltage dynamical thresholds to elicit an AP. These predictions agreed with our simulation results (Fig. 6 *D*) using the AP model.

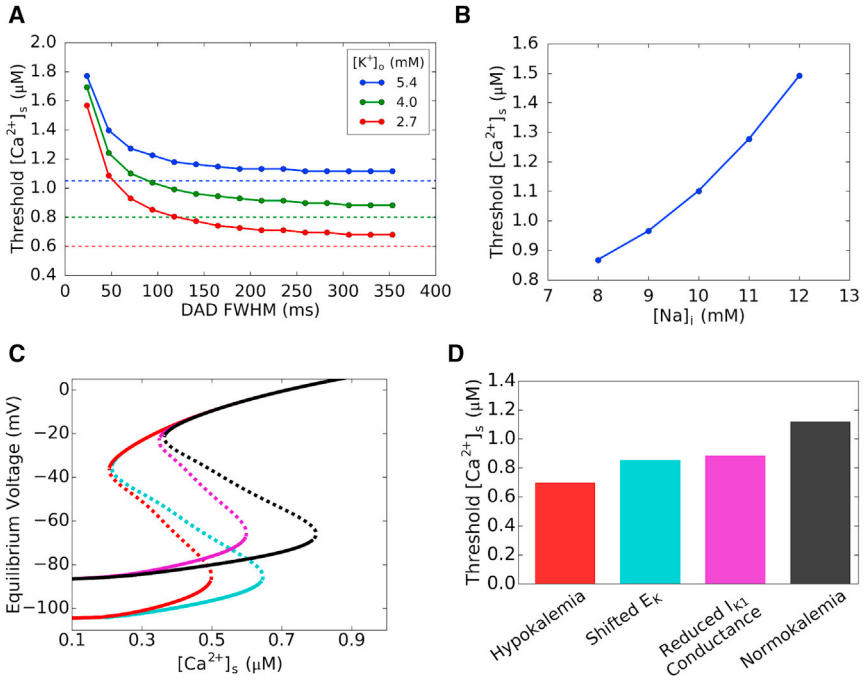

FIGURE 6 Submembrane Ca^{2+} transient thresholds for TA. (*A*) Ca^{2+} amplitude threshold for TA versus the FWHM of the Ca^{2+} transient and DAD for three different $[K]_o$ (5.4 mM *blue*, 4.0 mM *green*, and 2.7 mM *red*). (*Dashed lines*) Theoretical thresholds predicted using a three-current (I_{K1}, I_{NCX}, and I_{NaK}) system, with I_{NaK} adding a small quantitative increase in the outward current. Because the Ca^{2+} transient is a Gaussian function instead of a constant value, the Ca^{2+} threshold at steady state is slightly above the theoretically predicted values. (*B*) Ca^{2+} amplitude threshold for TA versus the intracellular Na^+ concentration $[Na^+]_i$. Lower $[Na^+]_i$ values result in a lower Ca^{2+} threshold. (*C*) Equilibrium voltage versus steady-state Ca^{2+} concentration under different conditions: control (*black*); reduced I_{K1} only (*magenta*); left-shifted E_K only (*cyan*); and hypokalemia (*red*). Note how the dynamical threshold shifts with each condition. (*D*) Ca^{2+} threshold results from simulations using the AP model under the same conditions in (*C*). Both the left shift of E_K as well as the reduced I_{K1} peak conductance lower the Ca^{2+} threshold to elicit an AP. This can be predicted by the different dynamical thresholds in each condition as seen in (*C*). To see this figure in color, go online.

TA and PVC suppression by blocking I_{Na}

The theoretical analyses above and experiments shown in Fig. 4 suggest that even in the absence of I_{Na}, the voltage will depolarize automatically beyond the $I_{Ca,L}$ threshold near −40 mV to elicit an AP as long as the Ca^{2+} amplitude and duration exceed the dynamical threshold. This implies that blocking I_{Na} may not be effective in suppressing TA. To demonstrate this effect, we carried out simulations in a single isolated myocyte by reducing the maximum conductance of I_{Na} from 12 mS/μF (the control value) to zero and determined the corresponding Ca^{2+} transient amplitude threshold for TA (Fig. 7 *A*). For normokalemia, the Ca^{2+} threshold increased slightly as g_{Na} was reduced from 12 to 6 mS/μF (the Ca^{2+} threshold was increased from 1.1 to 1.25 μM), then exhibited a faster increase as g_{Na} was reduced from 6 to 3 mS/μF (the Ca^{2+} threshold was increased from 1.25 to 1.6 μM), and then saturated as g_{Na} was finally reduced from 3 to 0 mS/μF. For hypokalemia ($[K^+]_o$ = 2.7 mM), the Ca^{2+} threshold remained almost the same until g_{Na} was reduced to 4 mS/μF from which the Ca^{2+} threshold was increased abruptly from 0.7 to 1.8 μM and then saturated. In both cases, the rapid increase in Ca^{2+} threshold as I_{Na} conductance decreases indicates the transition from an I_{Na}-mediated upstroke to a slower $I_{Ca,L}$-mediated upstroke, because it takes more time to reach the $I_{Ca,L}$ threshold. Fig. 7 *B* shows AP and Ca^{2+} traces when I_{Na} = 0.

Although these results demonstrated that I_{Na} is not necessary for TA in single myocytes, whether this is also true for TA-mediated PVCs in tissue was still unclear. To investigate the effect of I_{Na} block in cardiac tissue, we simulated a cable of 500 coupled myocytes with a central region of 40 cells exhibiting DADs of the same Ca^{2+} release strength but with different random latencies drawn from a Gaussian distribution (see Liu et al. (22) for more details of the method),

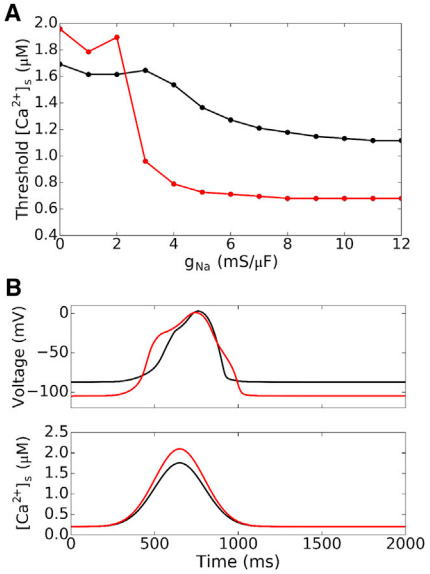

FIGURE 7 Effects of I_{Na} blockade on TA in a single isolated myocyte. (*A*) Submembrane Ca^{2+} transient threshold for TA versus g_{Na} in normokalemia (*black*) and hypokalemia (*red*). For most g_{Na} values, the Ca^{2+} threshold for TA is lower in hypokalemia than in normokalemia. (*B*) Voltage and Ca^{2+} traces for Ca^{2+} transients just above threshold with g_{Na} = 0, under normokalemic (*black*) and hypokalemic conditions (*red*). Due to the dynamical threshold automatically driving the voltage to the $I_{Ca,L}$ threshold, we still can elicit a slow upstroke AP with complete I_{Na} block. To see this figure in color, go online.

as in Fig. 8 *A*. For the control g_{Na} value (12 mS/μF), the conduction velocity for AP conduction is ~0.05 cm/ms for normokalemia and 0.042 cm/ms for hypokalemia, which decreases as g_{Na} is lowered until $g_{Na} = 3$ mS/μF, after which conduction completely fails (Fig. 8 *B*). As expected, hypokalemia reduces excitability and thus slows conduction.

We then calculated the probability of a PVC occurring in the cable at different levels of g_{Na} in normokalemia and hypokalemia (Fig. 8 *C*). For control g_{Na} with this distribution of Ca^{2+} release strengths, the probability of PVC is ~65% in normokalemia but almost 100% in hypokalemia. In normokalemia, the probability of PVC decreased as I_{Na} decreased, which drops to near zero at $g_{Na} = 3$ mS/μF. In hypokalemia, however, the probability of PVC exhibited almost no change until g_{Na} was reduced to 3 mS/μF and then dropped rapidly to zero at $g_{Na} = 2$ mS/μF. In both cases, the probability of PVC became zero only when I_{Na} is too small ($g_{Na} = 2$ mS/μF) to support conduction at all in the cable (Fig. 8 *B*). Note that we used the same Ca^{2+} release strength for both hypokalemia and normokalemia, and because the Ca^{2+} threshold in hypokalemia is much lower than in normokalemia, the peak Ca^{2+} values were already much higher than the TA threshold in hypokalemia. Because of this, the Ca^{2+} transient in hypokalemia is strong enough to depolarize the voltage in the DAD region above the threshold for TA no matter how much I_{Na} is available, as long as there is enough I_{Na} strength for successful conduction ($g_{Na} > 2$ mS/μF). If one used a lower Ca^{2+} release strength distribution, the probability of PVC would have a stronger dependence on I_{Na}, as shown in the normokalemia case. Therefore, at the tissue-scale, blocking I_{Na} can still suppress Ca^{2+}-mediated PVCs as long as the Ca^{2+} transient is not much higher than the Ca^{2+} threshold for TA.

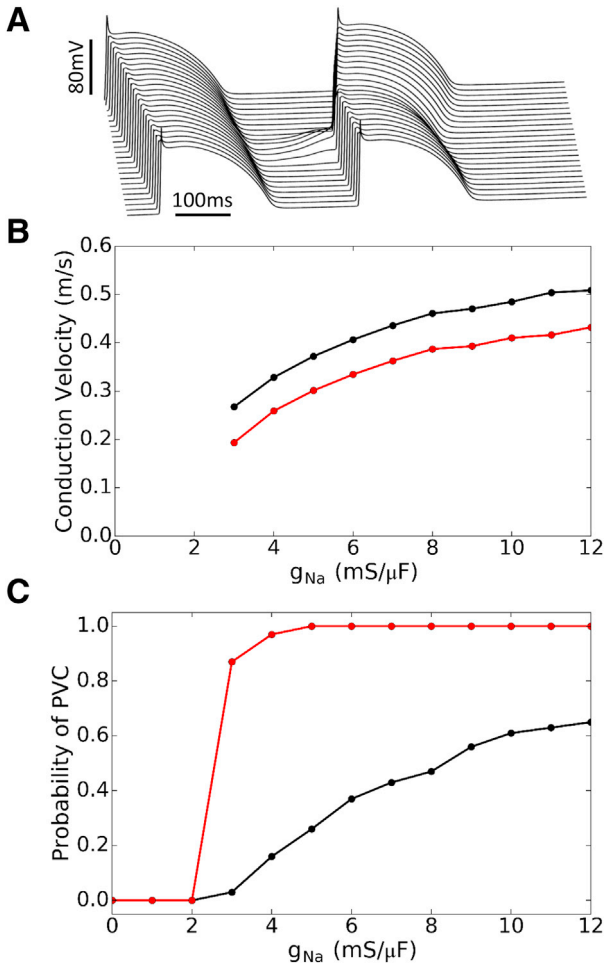

FIGURE 8 Suppression of PVCs in tissue by I_{Na} blockade. (*A*) Representative voltage traces for a 1D cable of 200 cells with a region of 40 cells in the center exhibiting DADs with a release strength $g_{spon} = 0.250$ ms^{-1} whose random latencies were drawn from a Gaussian distribution with time to onset $t_{0,onset} = 300$ ms and standard deviation $\sigma_{latency} = 50$ ms. See Liu et al. (22) for details. Note also that in Liu et al. (22), t_0 corresponds to the Ca^{2+} release onset ($t_{0,onset}$), not the Ca^{2+} transient peak as in this article. This particular example shows a paced beat propagating through the entire cable, followed by the central region exhibiting suprathreshold DADs that trigger a propagating PVC. (*B*) Conduction velocity versus g_{Na} for normokalemia (*black*) and hypokalemia (*red*). Conduction failure occurs for $g_{Na} < 3$ mS/μF. (*C*) The probability of PVC occurring in the cable (100 random simulations per data point) versus g_{Na} for normokalemia (*black*) and hypokalemia (*red*). For a fixed strength of spontaneous Ca^{2+} release in the DAD region, the probability of PVCs gradually decreased with lowered g_{Na} in normokalemia, but remained high in hypokalemia until conduction failure occurred. To see this figure in color, go online.

DISCUSSION

In this study, we investigated the voltage threshold for eliciting an AP by current pulses and DADs in ventricular myocytes. We show that a short current pulse must provide enough charge movement to directly depolarize the membrane potential to the I_{Na} threshold near −60 mV to elicit a rapid AP upstroke. Therefore, when the resting potential is hyperpolarized and lies further away from the I_{Na} threshold, such as during hypokalemia, a stronger stimulus is required to elicit an AP, i.e., the excitability of a myocyte is reduced and conduction velocity in tissue is slower (1–3). However, during a long current pulse or a DAD, the threshold for triggering an AP is different. While the membrane voltage must eventually reach the I_{Na} threshold to trigger a rapid AP upstroke, the true threshold for TA is a dynamical threshold. In the case of a DAD, this dynamical threshold is mainly determined by I_{K1} and I_{NCX} (with I_{NaK} adding a small quantitative contribution, ~20% of the effective peak I_{K1}) manifesting as a saddle-node bifurcation in which the dynamical threshold is the bifurcation point. The dynamical threshold occurs at a lower voltage than the I_{Na} threshold during both normokalemia and hypokalemia. Once intracellular Ca^{2+} rises and activates sufficient I_{NCX} to depolarize the myocyte past the dynamical threshold, the voltage continues to automatically depolarize to above the I_{Na} threshold due to a steep negative slope of the I_{K1}-V curve. Thus, despite decreased excitability in response to short current pulses, DAD-mediated TA is

facilitated by hypokalemia due to the lower dynamical threshold. The nonlinear dynamical analysis shows that the lower dynamical threshold results from a reduced I_{K1} conductance, a well-known factor that promotes (DAD)-mediated TA (6–8), and from a left shift of $E_{K,}$ such that a smaller Ca^{2+} transient is able to induce TA. Thus, the lower dynamical threshold interacts synergistically with another key effect of hypokalemia, Na^{+}-K^{+} pump inhibition causing intracellular Ca^{2+} overload (16,17) and spontaneous diastolic Ca^{2+} release, to promote DAD-mediated TA. Because the voltage can automatically depolarize above the I_{Na} threshold to reach $I_{Ca,L}$ threshold after passing the saddle-node bifurcation point (or the dynamical threshold), triggered APs can occur in single myocytes in the absence of I_{Na}, suggesting that blocking I_{Na} may not be effective at suppressing TA. However, because I_{Na} is important for AP propagation in tissue, blocking I_{Na} can still suppress PVCs in cardiac tissue caused by Ca^{2+}-mediated TA.

Our findings expand on the previous work of Greene and Shiferaw (18), who demonstrated analytically that the threshold for AP excitation caused by a steady-state constant current pulse is lower than the I_{Na} threshold near the voltage at which I_{K1} is maximum. In addition to experimentally validating this prediction in isolated myocytes and extending the findings to hypokalemia, we performed a detailed analysis of the nonlinear dynamics for DAD-mediated TA by considering a simple system incorporating the two currents most important in determining diastolic voltage, i.e., the I_{K1}-I_{NCX} system. We showed that the two-current system can exhibit bistability and undergoes a saddle-node bifurcation that determines the dynamical threshold. Besides the existence of a dynamical threshold, the nonlinear dynamics also predicts the following:

1) Once the voltage is above the dynamical threshold, the Ca^{2+} concentration does not necessarily need to increase further to depolarize the voltage to the I_{Na} threshold. The voltage can still automatically depolarize further even if Ca^{2+} decreases during this phase (Fig. 5 *C*), as long as the rate of decrease in I_{NCX} is not faster than the decrease in I_{K1} as voltage rises to the I_{Na} threshold.
2) The position of the upper equilibrium point is an important factor governing the automatic phase of depolarization beyond the dynamical threshold, affecting the efficiency at which the myocyte reaches the I_{Na} or $I_{Ca,L}$ threshold. Note that in the constant stimulus current case as analyzed in this study and by Greene and Shiferaw (18), the upper equilibrium point does not exist. The upper equilibrium is mainly determined by I_{NCX}. It is obvious that the higher the upper equilibrium, the easier for the system to depolarize to the I_{Na} or $I_{Ca,L}$ threshold. For example, increasing the magnitude of I_{NCX} (by simply increasing the I_{NCX} amplitude) has little effect on elevating the upper equilibrium point (although it can have an effect on lowering the dynamical threshold) because this only tilts the I_{NCX} curve more steeply to affect the saddle-node bifurcation point. In contrast, increasing Ca^{2+} concentration can have a large effect on both the dynamical threshold and the upper equilibrium point, because in addition to tilting I_{NCX}, a larger Ca^{2+} also shifts the I_{NCX} curve to the right, increasing the margin between the I_{NCX} and I_{K1} curves. This steep tilt and right shift of I_{NCX} effectively makes it easier to depolarize the voltage above the I_{Na} or $I_{Ca,L}$ threshold. Similarly, reducing I_{K1} conductance can also lower the dynamical threshold but will have little effect on the upper equilibrium point.

In conclusion, using nonlinear dynamics and patch-clamp experiments, we have demonstrated the existence of a dynamical threshold for DAD-mediated TA, which is lower than the I_{Na} threshold. The dynamical threshold is further lowered by hypokalemia, facilitating DAD-mediated TA by hypokalemia. Our dynamical analysis and computer simulation have demonstrated distinct roles of Ca^{2+}, I_{K1}, I_{NCX}, and I_{Na} in potentiating DAD-mediated TA, which not only provide important insights into the mechanism of DAD-mediated TA but also useful information for future development of antiarrhythmic therapies.

AUTHOR CONTRIBUTIONS

M.B.L., Z.S., J.N.W., and Z.Q. conceived the study; M.B.L. and Z.Q. developed the theory, designed the simulations, and wrote the article; M.B.L. performed the simulations; C.Y.K. and J.N.W. designed and performed the experiments; and all authors analyzed the data and commented on the article.

ACKNOWLEDGMENTS

Supported by National Heart, Lung and Blood Institute grant No. P01 HL078931; UCLA MCIP institutional training grants No. T32 GM065823 (to M.B.L.) and No. T32 HL07895 (to C.Y.K.); American Heart Association predoctoral fellowship No. 16PRE27610040 (to M.B.L.); and the Laubisch and Kawata endowments.

REFERENCES

1. Kagiyama, Y., J. L. Hill, and L. S. Gettes. 1982. Interaction of acidosis and increased extracellular potassium on action potential characteristics and conduction in guinea pig ventricular muscle. *Circ. Res.* 51:614–623.
2. Shaw, R. M., and Y. Rudy. 1997. Electrophysiologic effects of acute myocardial ischemia. A mechanistic investigation of action potential conduction and conduction failure. *Circ. Res.* 80:124–138.
3. Xie, Y., A. Garfinkel, …, Z. Qu. 2009. Effects of fibroblast-myocyte coupling on cardiac conduction and vulnerability to reentry: a computational study. *Heart Rhythm.* 6:1641–1649.
4. Miake, J., E. Marbán, and H. B. Nuss. 2002. Biological pacemaker created by gene transfer. *Nature.* 419:132–133.
5. Silva, J., and Y. Rudy. 2003. Mechanism of pacemaking in I_{K1}-down-regulated myocytes. *Circ. Res.* 92:261–263.

6. Schlotthauer, K., and D. M. Bers. 2000. Sarcoplasmic reticulum Ca^{2+} release causes myocyte depolarization. Underlying mechanism and threshold for triggered action potentials. *Circ. Res.* 87:774–780.
7. Pogwizd, S. M., K. Schlotthauer, …, D. M. Bers. 2001. Arrhythmogenesis and contractile dysfunction in heart failure: roles of sodium-calcium exchange, inward rectifier potassium current, and residual β-adrenergic responsiveness. *Circ. Res.* 88:1159–1167.
8. Maruyama, M., B. Joung, …, P. S. Chen. 2010. Diastolic intracellular calcium-membrane voltage coupling gain and postshock arrhythmias: role of Purkinje fibers and triggered activity. *Circ. Res.* 106:399–408.
9. Rosen, M. R., J. P. Moak, and B. Damiano. 1984. The clinical relevance of afterdepolarizations. *Ann. N. Y. Acad. Sci.* 427:84–93.
10. January, C. T., and H. A. Fozzard. 1988. Delayed afterdepolarizations in heart muscle: mechanisms and relevance. *Pharmacol. Rev.* 40:219–227.
11. Marban, E., S. W. Robinson, and W. G. Wier. 1986. Mechanisms of arrhythmogenic delayed and early afterdepolarizations in ferret ventricular muscle. *J. Clin. Invest.* 78:1185–1192.
12. Ter Keurs, H. E. D. J., and P. A. Boyden. 2007. Calcium and arrhythmogenesis. *Physiol. Rev.* 87:457–506.
13. Katra, R. P., and K. R. Laurita. 2005. Cellular mechanism of calcium-mediated triggered activity in the heart. *Circ. Res.* 96:535–542.
14. Yeh, Y. H., R. Wakili, …, S. Nattel. 2008. Calcium-handling abnormalities underlying atrial arrhythmogenesis and contractile dysfunction in dogs with congestive heart failure. *Circ. Arrhythm. Electrophysiol.* 1:93–102.
15. Morita, H., D. P. Zipes, …, J. Wu. 2007. Mechanism of U wave and polymorphic ventricular tachycardia in a canine tissue model of Andersen-Tawil syndrome. *Cardiovasc. Res.* 75:510–518.
16. Pezhouman, A., N. Singh, …, J. N. Weiss. 2015. Molecular basis of hypokalemia-induced ventricular fibrillation. *Circulation.* 132:1528–1537.
17. Aronsen, J. M., J. Skogestad, …, I. Sjaastad. 2015. Hypokalaemia induces Ca^{2+} overload and Ca^{2+} waves in ventricular myocytes by reducing Na^{+},K^{+}-ATPase α2 activity. *J. Physiol.* 593:1509–1521.
18. Greene, D., and Y. Shiferaw. 2015. Approximate analytical solutions for excitation and propagation in cardiac tissue. *Phys. Rev. E Stat. Nonlin. Soft Matter Phys.* 91:042719.
19. Scaringi, J. A., A. O. Rosa, …, L. Cleemann. 2013. A new method to detect rapid oxygen changes around cells: how quickly do calcium channels sense oxygen in cardiomyocytes? *J. Appl. Physiol.* 115:1855–1861.
20. Mahajan, A., Y. Shiferaw, …, J. N. Weiss. 2008. A rabbit ventricular action potential model replicating cardiac dynamics at rapid heart rates. *Biophys. J.* 94:392–410.
21. Xie, Y., D. Sato, …, J. N. Weiss. 2010. So little source, so much sink: requirements for afterdepolarizations to propagate in tissue. *Biophys. J.* 99:1408–1415.
22. Liu, M. B., E. de Lange, …, Z. Qu. 2015. Delayed afterdepolarizations generate both triggers and a vulnerable substrate promoting reentry in cardiac tissue. *Heart Rhythm.* 12:2115–2124.
23. Baer, M., P. M. Best, and H. Reuter. 1976. Voltage-dependent action of tetrodotoxin in mammalian cardiac muscle. *Nature.* 263:344–345.
24. Cohen, C. J., B. P. Bean, …, R. W. Tsien. 1981. Tetrodotoxin block of sodium channels in rabbit Purkinje fibers. Interactions between toxin binding and channel gating. *J. Gen. Physiol.* 78:383–411.
25. Carmeliet, E. 1987. Voltage-dependent block by tetrodotoxin of the sodium channel in rabbit cardiac Purkinje fibers. *Biophys. J.* 51:109–114.
26. Strogatz, S. H. 2000. Nonlinear Dynamics and Chaos: with Applications to Physics, Biology, Chemistry, and Engineering. Westview Press, Cambridge, UK.
27. Ko, C. Y., Z. Song, …, J. N. Weiss. 2015. Multiscale consequences of spontaneous calcium release on cardiac delayed afterdepolarizations. *Biophys. J.* 108:264a.